Hydrogels Derived from Lignin with pH Responsive and Magnetic Properties

Wu Liu, Zhihui Ye, Dexiang Liu, and Zhiping Wu *

Smart lignin hydrogels with pH responsive and magnetic properties was prepared by free radical polymerization from lignin and acrylamide. In order to improve its swelling properties, calcium carbonate as pore-foaming agent was introduced to the polymer formulation, then magnetic particles (Fe_3O_4) was formed in the polymer by *in situ* reaction and co-precipitation. The results showed that degree of swelling of pH responsive hydrogels (PLH) containing the pore-foaming agent increased 47% compared to the original hydrogels (OLH) without pore-foaming agent, and the swelling rate of PLH reached 100% within 13.5 min under optimum pH conditions (pH = 6.8) which is a shorter amount of time, 1.5 times, compared to the OLH. The swelling-deswelling experiments showed that the hydrogels retained good reversibility and stability. Fourier transform infrared (FTIR) spectra indicated that the molecular chain of the PAM matrix hydrogels was successfully grafted on the lignin and the magnetic particles (Fe_3O_4) precipitated in the hydrogel. The X-ray diffraction (XRD) results showed that the magnetic particles in the hydrogels were composed of magnetite. The presence of a mesoporous structure was observed in scanning electron microscopy (SEM) images. The composition of hydrogels was analyzed by energy dispersive spectroscopy (EDS). The vibrating sample magnetometer (VSM) measurements also showed good magnetic properties.

Keywords: Lignin; pH responsive; Magnetic properties; Hydrogels; Swelling

*Contact information: School of Materials Science and Engineering, Central South University of Forestry and Technology, Changsha 410004, China; *Corresponding author: wuzhiping02@163.com*

INTRODUCTION

With the increasing petrochemical crisis and environmental pollution, biomass resources have attracted much attention towards developing alternatives to objects and parts presently prepared from petrochemicals. Lignin is the second most abundant biopolymer on earth. Lignin is an aromatic compound of phenylpropane that exhibits tremendous potential for refining to obtain compounds and fuels that presently are obtained from petrochemicals (Liu *et al.* 2017; Peng *et al.* 2015; Zhang 2012). However, it has been largely underutilized as low value power through incineration due to its complicated structure (Chen *et al.* 2016). Lignin possesses a large number of active groups and high chemical reactivity. Thus, the petroleum base was partially replaced by lignin to create intelligent composite materials (Gutiérrez-Hernández *et al.* 2016; Marcelo *et al.* 2016; Spasojević *et al.* 2016). Functions of smart composite that have been reported include temperature responsive, pH responsive, ion responsive, electrical responsive, magnetic responsive, and light responsive (Kai *et al.* 2015; Wan and Li 2015; Shen *et al.* 2016). They are mostly applied to fields relating to bionics, memory materials, super capacitors, super absorbent materials, and controlled-release drug carriers (Oroumei *et al.* 2015; Eslahi *et al.* 2016).

The pH-responsive intelligent materials, including membranes, microspheres, microcapsules, and hydrogels, play an important role in the field of drug release, heavy metal adsorption, and separation materials (Feng *et al.* 2014; Ji *et al.* 2017). In recent years, multifunctional, selective, recyclable, and biodegradable hydrogels have received widespread attention (Jin *et al.* 2017; Wang *et al.* 2017). More importantly, lignin-grafted polyacrylamide (PAM) matrix hydrogels meet the above requirements. The responsive hydrogels contain a large number of hydrophilic groups that are easy to hydrolyze or protonate. At the same time, the three-dimensional structure of hydrogels can be changed with the different pH of the liquid medium, resulting in the change of the volume of hydrogels. Meanwhile, lignin contains a large number of phenolic hydroxyl and carboxyl groups that can greatly enhance the degree of ionization. Changes in pH will change the dissociation and ionic concentration inside and outside the hydrogel, and such changes can form or break hydrogen bonds in the grid. The responsive time of hydrogels is one of the most important parameters (Ragauskas *et al.* 2014). Under normal circumstances, responsive behavior is needed for hydrogels to achieve efficient adsorption. Fast responsive thermosensitive poly (N-N-isopropylacrylamide) (PNIPA) hydrogels were synthesized by using a pore-foaming agent ($CaCO_3$), and the swelling rate increased up to 100% in 40 min. The porosity and specific surface area of the hydrogels increased using the pore-foaming agent. Meanwhile the swelling and dehydration of the hydrogels were greatly enhanced (Liu *et al.* 2002).

Iron oxide magnetic materials have drawn much attention owing to their tremendous potential field of targeted drug delivery, tumor hyperthermia, genetic engineering, sewage purification, and catalysis (Shen *et al.* 2014; Xu *et al.* 2015; Sun *et al.* 2016). Chitosan-coated magnetic adsorbents were prepared by co-precipitation method and used for removing Cr(VI) from wastewater. The 96.3% of Cr (VI) was absorbed by magnetic chitosan with the optimum conditions (Ravi and Jabasingh 2017).

Herein, the authors synthesized pH responsive and magnetic hydrogels with recyclable, biodegradable, and multifunctional *via* chemical co-precipitation and pore-foaming agent (Scheme 1). First, lignin was purified by sulfuric acid. Then, pore-foaming agent and acrylamide (AM) were prepared into porous hydrogels. Finally, chemical co-precipitation was synthesized *in situ* magnetic particles. (Fig. 1) (Liu *et al*. 2002; Chung *et al.* 2013; Liu *et al.* 2013).

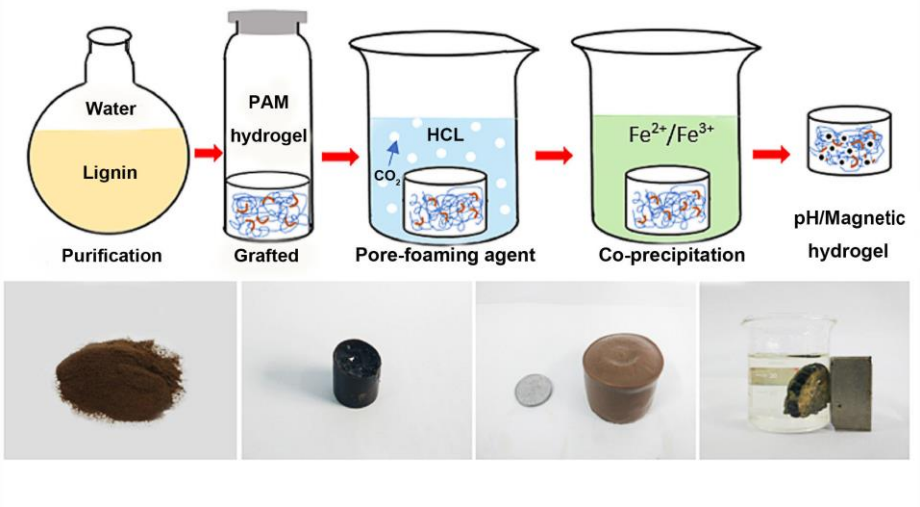

Fig. 1. Preparation of pH responsive and magnetic hydrogels *via* pore-foaming agent and co-precipitation methods

EXPERIMENTAL

Materials

Lignin was purchased from Shanghai Shun Zhan Chemical Co., Ltd., Shanghai, P. R. China and it is the byproduct of the alkaline pulping from hardwood. The phenolic hydroxyl and carboxyl content of lignin was measured to be 3 and 7 mmol/g, respectively. The acrylamide, the solvent: dimethyl sulfoxide (DMSO), the crosslinking agent: ethylene glycol dimethyl acrylate (EGDMA), 98% sulfuric acid (H_2SO_4), sodium chloride (NaCl), the initiator: 30% hydrogen peroxide (H_2O_2) and calcium chloride ($CaCl_2$), iron (Ⅲ) chloride ($FeCl_3$), iron (Ⅱ) sulfate heptahydrate ($FeSO_4 \cdot 7H_2O$), the pore-foaming agent: calcium carbonate ($CaCO_3$), sodium hydroxide (NaOH) and 37% hydrochloric acid (HCl) used in this work were analytical reagent and purchased from Tianjin Chemical Plant, Tianjin, P. R. China.

Purification of lignin

Impurities in the original material, such as inorganic salt, reducing sugar, and hemicellulose, not only react with lignin but also decrease the crosslinking degree of the hydrogel under acidic conditions (Mir *et al.* 2014; Nair *et al.* 2014). Therefore, purification of lignin is essential. First, 10 g lignin powders were placed in a beaker at room temperature and completely dissolved by deionized water with stirring. After vacuum filtration, the filtrate was mixed with 64 mL 98% H_2SO_4 and stirred at 80 °C for 4 h. When the reacted solution cooled to room temperature, 100 g NaCl was added and stirred for 1 h before being filtered by a sand funnel; then it was dried under 40 °C in vacuum drying oven until the weight was constant (Feng *et al.* 2014).

Preparation of magnetic particles

Magnetic particles (M) were prepared by chemical precipitation. The molar ratio of the aqueous solution of iron (Ⅱ) sulfate heptahydrate ($FeSO_4 \cdot 7H_2O$) and iron (Ⅲ) chloride ($FeCl_3$) is 1:2, mixed in a 30 mL glass bottle with nitrogen gas protection under room temperature, then 0.1 M sodium hydroxide (NaOH) solution was charged into the bottle and reacted one hour. The coprecipitated product was filtered and dried under 40 °C for 6 h in vacuum drying oven.

Preparation of pH responsive and magnetic lignin hydrogels

Original hydrogels (OLH), pH responsive hydrogels (PLH), and pH responsive and magnetic hydrogels (MPLH) were prepared in order to compare the effect of pore-foaming agent and magnetism. First, at room temperature, the purified lignin, acrylamide (AM), $CaCl_2$, DMSO, and the $CaCO_3$ were fully stirred and transferred into a 30 mL glass bottles. Then, the cross-linking agent EGDMA and initiator H_2O_2 (content 30%) were added to the above solution. The specific ratio is shown in Table 1. Finally, the mixed solution was sealed with nitrogen for 20 min and reacted for 12 h at 70 °C. After the reaction, the hydrogel was placed in 1 M HCl solution for 12 h under ambient temperature and dried in a vacuum oven at 40 °C until the weight was constant (Segtnan *et al.* 2006). The dried hydrogels were immersed in a solution of seven hydrated ferrous sulfate ($FeSO_4 \cdot 7H_2O$) and ferric chloride ($FeCl_3$) (molar ratio is 1:2) for 12 h. Then, the hydrogels were reacted with 0.1 M NaOH solution for 1 h. Finally, the unreacted NaOH was washed away by deionized water and the hydrogel was vacuum dried.

Table 1. Feed Composition for the Preparation of the Lignin Hydrogels

Samples	Lignin (g)	$CaCl_2$ (g)	AM (g)	DMSO (mL)	H_2O_2 (uL)	EGDMA (uL)	$CaCO_3$ (g)	Mix-Fe (g)
OLH	0.5	0.4	3.5	4	5	32	0	0
PLH	0.5	0.4	3.5	4	5	32	0.6	0
MPLH	0.5	0.4	3.5	4	5	32	0.6	6.5

Methods

Characterization

The hydrogels' group tests were carried out with the NEXUS870 Fourier transform infrared spectrometer (FTIR; Nicolet, Madison, WI, USA). The lignin, hydrogels (OLH, PLH and MPLH), and magnetic particles (M) dried powder were tableted by KBr and their functional groups were analyzed by infrared spectroscopy. The wavelength coverage was 400 cm^{-1} to 4000 cm^{-1}.

The crystallization property of lignin, hydrogels (OLH, PLH, and MPLH) and magnetic particles (M) was tested *via* a D8 ADVANCE X-ray diffractometer (XRD; Bruker, Karlsruhe, Germany). The test of samples were characterized to investigate the crystal structure in materials. The test condition was continuous scanning, the step size was 0.02°, the scanning speed was 2°/min, the scanning range was 5° to 90°, the working voltage was 40 kV, and the working current was 40 mA.

The morphology and elements of hydrogel were analyzed with a Quanta 450 scanning electron microscope (SEM; FEI Company, Hillsboro, OR, USA) and INCA X-ACT 25° energy dispersive spectroscopy (EDS; Oxford instruments, Oxford, London, UK). The OLH, PLH, and MPLH swelled until equilibrium state in deionized water. Then, it was frozen in a refrigerator at -18 °C for 12 h. The whole frozen hydrogels were freeze-dried for 3 d. The freeze-dried hydrogels, lignin powder and magnetic particles (M) were sprayed with gold (Quorum, East Sussex, UK) and observed under the scanning electron microscope and energy dispersive spectroscopy.

The magnetic properties of the hydrogel (MPLH) and magnetic particles (M) were analyzed by a PPMS-9 Design Quantum Magnetometer (VSM; Quantum Design, San Diego, CA, USA). Testing conditions were as follows: temperature 300 K, variation magnetic field strength 0 Oe to 20000 Oe. The hysteresis loops were obtained.

pH responsive and swelling-deswelling test of hydrogel

Three kinds of dried hydrogels, OLH, PLH, and MPLH, were placed in buffer solution with pH value of 4.00, 6.86, and 9.18, respectively. These hydrogels were dried and weighed after 12 hours. Swelling of hydrogels was calculated according to Eq. 1,

$$\mathrm{w} = \frac{M_m - M_o}{M_o} \quad (1)$$

where W (%) is the swelling rate of hydrogels, M_m (g) is the mass of swollen hydrogels, and M_o (g) is the mass of original hydrogels .

The grain size of M and MPLH grains was calculated by XRD data by Debye-Scherrer formula (2),

$$D = \frac{K\gamma}{B\cos\theta} \quad (2)$$

where K (K=0.89) is Scherrer constant and B is half peak width of XRD peak of the measured sample; D is the average thickness of the sample grain in the direction of crystal plane (nm); and θ is the diffraction angle of the XRD peak. The parameter γ (γ=0.154056) is the wavelength of X rays.

RESULTS AND DISCUSSION

Preparation of pH-responsive and Magnetic Lignin Hydrogels

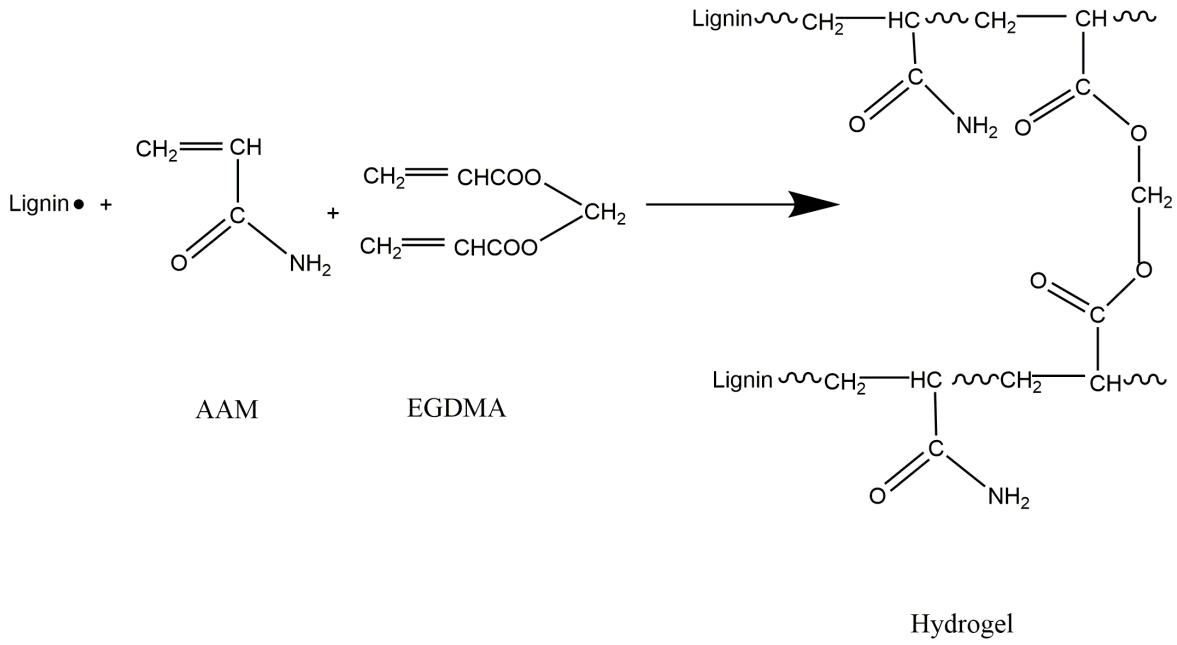

Fig. 2. Preparation of pH-responsive lignin hydrogels

Figure 2 shows the PLH reaction formula for PAM matrix hydrogel chain grafted onto lignin. The reaction mechanism is that H_2O_2/$CaCl_2$ initiate the formation of free radicals on lignin and copolymerize with acrylamide under the action of crosslinking agent EGDMA (Feng *et al.* 2014).

MPLH was prepared by *in situ* reaction and co-precipitation. The isoelectric point of Fe_3O_4 particles is 6.4. The preparation process was completed under alkaline conditions and showed negative electricity of M. At the same time, the carboxyl group produced by the hydrolysis reaction of amides in PLH and the phenolic hydroxyl group and carboxyl group on lignin are both electronegative. Thus, the formation of hydrogen bonds helps particles to precipitate on PLH to prepare MPLH.

Infrared Spectrum of Hydrogel

The functional groups of lignin, magnetic particles (M), and hydrogels (OLH, PLH and MPLH) were analyzed by Fourier transform infrared spectroscopy, and the results are shown in Fig. 3. Characteristic peak of asymmetric and symmetric stretching vibrations of N-H were located at 3415 cm^{-1} and 3191 cm^{-1}, respectively. The absorbance at 3415 cm^{-1} of lignin that was assigned to vibration of O-H was overlapped with N-H asymmetric vibration. The characteristics absorption peak of C=O were observed at 1660 cm^{-1}, which

indicated that these three kinds of hydrogel matrix material of polyacrylamide did not change. The absorption peaks at 1406 cm^{-1}, 1590cm^{-1}, and 1119 cm^{-1} represented the aliphatic groups, the skeleton vibrational absorption peak, and vibrational absorption peaks of aromatic rings of lignin, respectively. This indicated that these three kinds of hydrogels had been successfully introduced into the lignin. When magnetic particles are introduced into PLH, the characteristic peak of PLH is weakened while the M is enhanced in the MPLH spectrogram. We used XRD, EDS, and VSM detection methods to further verify the existence of magnetic particles. (Xiang *et al.* 2015).

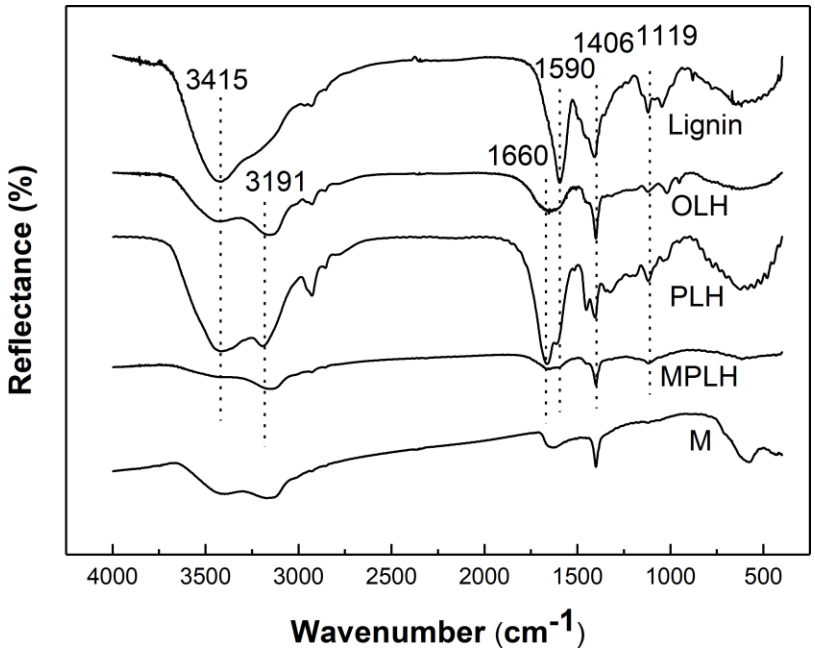

Fig. 3. FTIR spectra of lignin, hydrogels (OLH, PLH, and MPLH), and magnetic particles (M)

X-ray Diffraction Analysis of Hydrogel

The crystal structure of lignin, magnetic particles (M), and hydrogels (OLH, PLH, and MPLH) was analyzed by XRD, and the XRD spectrum is presented in Fig. 4. As shown, the lignin, OLH, and PLH were amorphous structures, and only characteristic diffraction peaks appeared in the diffraction angle (2θ) 20° to 30°. This indicated that lignin, OLH, and PLH were amorphous and consisted of a small amount of loosely structured crystals. The apparent diffraction peak in lignin samples may be due to the remaining inorganic salt crystals in the preparation of the original material. The multiple diffraction peaks appeared on the spectral line of M and MPLH. The major peaks corresponded to (220), (311), (400), (422), (511), and (440) crystal planes, which coincided with the standard characteristic diffraction peaks of type Fe_3O_4 (standard diffraction peak number 19-0629) particles and coincide with the results of Mir *et al.* (2014), indicating that the magnetic particles generated in the gel network were Fe_3O_4 particles. According to the Debye-Scherrer formula, the grain sizes of pure M and M containing MPLH were 8.5 nm and 10 nm, respectively.

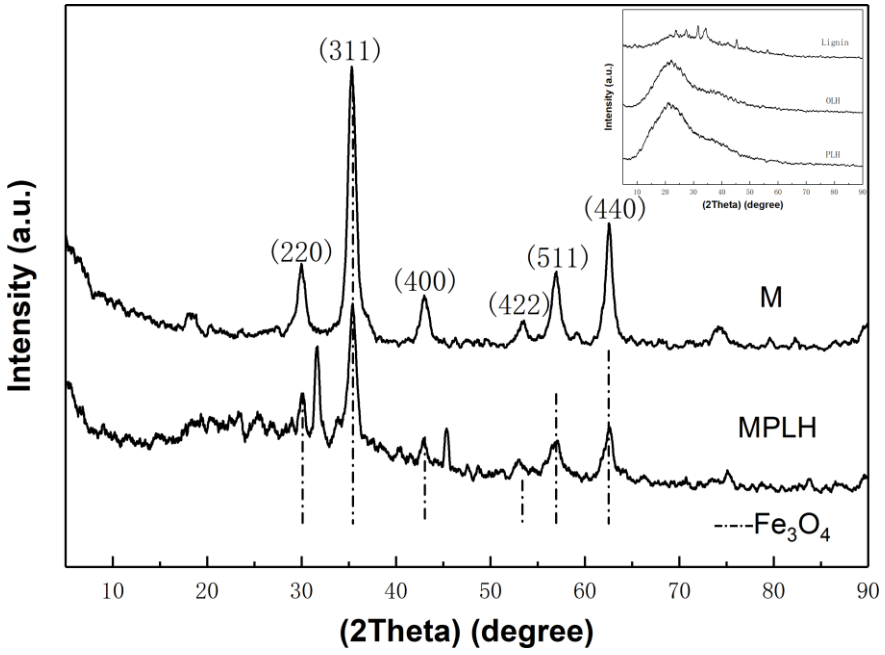

Fig. 4. XRD spectrum of lignin, magnetic particles (M), and hydrogels (OLH, PLH, and MPLH)

Hydrogel Morphology and Element Analysis

The morphologies of the three hydrogels were investigated by SEM. The photos of OLH, PLH, and MPLH are shown in Fig. 5. It can be seen that OLH without pore-foaming agent treatment had a relatively smaller pore size. However, the PLH with pore-foaming agent treatment improved pore structure, reaching a mesoporous level at approximately 10 μm.

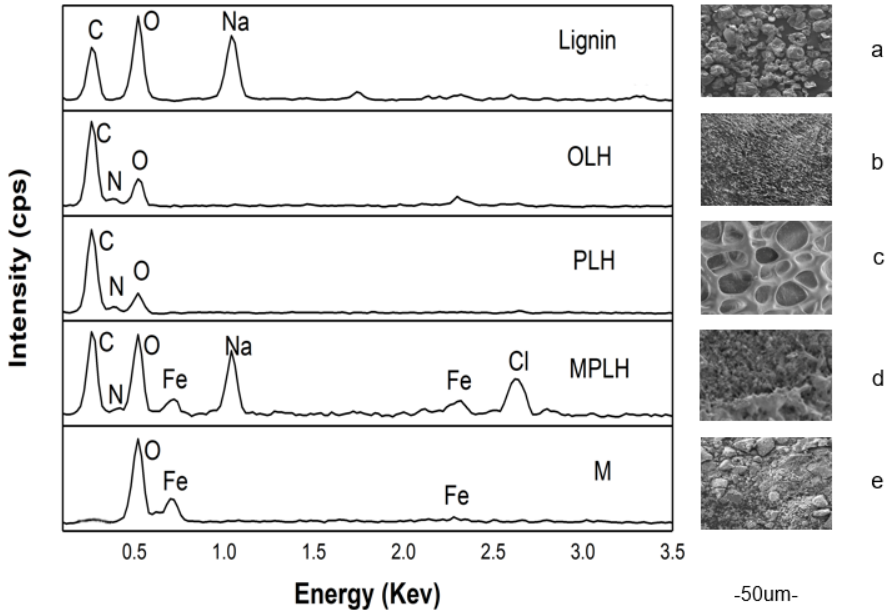

Fig. 5. SEM and EDS images of (a) lignin, (b) magnetic particles (M) and (c), (d), (e) hydrogels (OLH, PLH and MPLH)

Although the MPLH was also treated with pore-foaming agent, its pore was smaller than that of PLH. The generated Fe_3O_4 particles plugged the original pores, but the formation of Fe_3O_4 particles in NaOH solution also led to a certain degree of depolymerization of the hydrogels matrix, directly affecting the three-dimensional network structure of hydrogels matrix. Meanwhile, the composition of hydrogels was analyzed by energy dispersive spectroscopy (EDS). Figure 5 clearly shows the N presented in b, c, and d and is caused by the addition of the amide group. The comparison between c and d in Fig. 5 shows that the iron element in MPLH appeared because magnetic particles Fe_3O_4 are deposited in the hydrogel.

Magnetic Properties of Hydrogels

The hysteresis loop of MPLH and M was tested *via* VSM, and the results are presented in Fig. 6. The dried PLH adsorbed mixed iron salts and generated Fe_3O_4 particles in the hydrogel by *in situ* precipitation method, therefore giving the hydrogel magnetic properties. Hysteresis was not observed from the hysteresis loop, indicating that the sample had paramagnetic properties. The value of remanence and coercivity were both zero and the particle size was smaller than the critical size, which indicated that the generated Fe_3O_4 is superparamagnetic. Therefore, the hydrogel also is superparamagnetic and its apparent saturation magnetization was 6.63 emu g^{-1}. We have also added experiments to compare the magnetic properties of magnetic particles and magnetic hydrogels. It is found that the saturation magnetization of hydrogels was obviously lower than that of magnetic particles, which is due to the decrease of saturation magnetization due to the agglomeration of magnetic particles and the decrease of the content (Li *et al.* 2014).

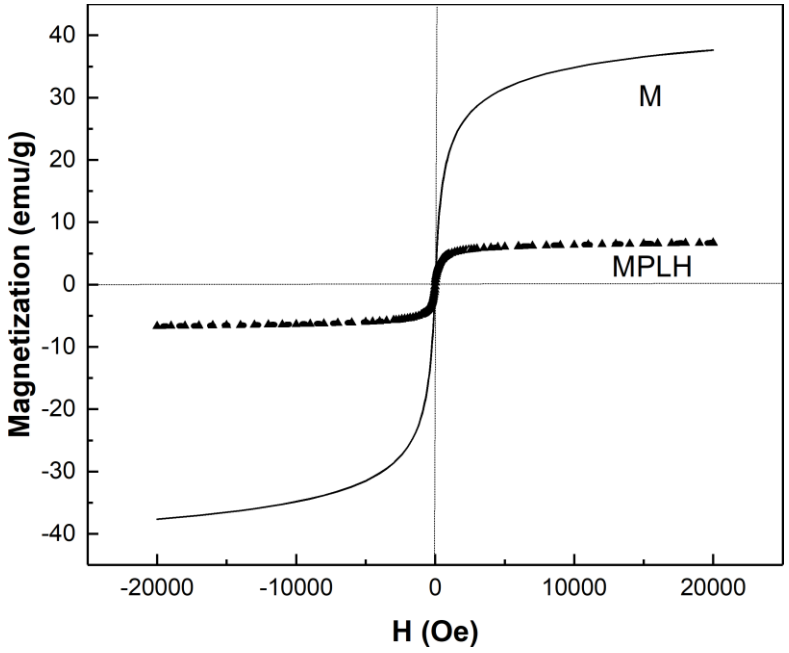

Fig. 6. Magnetization curve of MPLH and M

pH Responsive Tests of Hydrogels

The pH responsive of hydrogels are mainly caused by the change of weak electrolyte groups responding to stimulus from the environment. The amide group of the acrylamide hydrogel has good pH sensitivity. The lignin itself carries a large amount of

phenolic hydroxyl groups and carboxyl groups onto the hydrogel matrix, promoting the pH-responsive properties of the hydrogel by synergistic action. The change of pH-responsive properties of three hydrogels under various pH (4.00, 6.86, and 9.18) is shown in Fig. 7. When pH value is low, the anionic groups of phenol hydroxyl and carboxyl in hydrogel form hydrogen bond. The increased force between the molecular chains limits the movement of the polymer chains. Finally, a tight hydrogel network structure was formed, which resulted in a low swelling rate of hydrogel. When the pH value rises from 4.00 to 6.86, the ionization degree and the number of internal fixed charges in the hydrogel increase, resulting in the weakening of hydrogen bonding force and the increase of internal ion concentration. At this time, the structure of hydrogel is loose and swelling ability is enhanced. When the pH value is further increased, the hydrogel is depolymerized under alkaline conditions, and its structure is destroyed and its swelling ability is greatly weakened (Song *et al.* 2014).

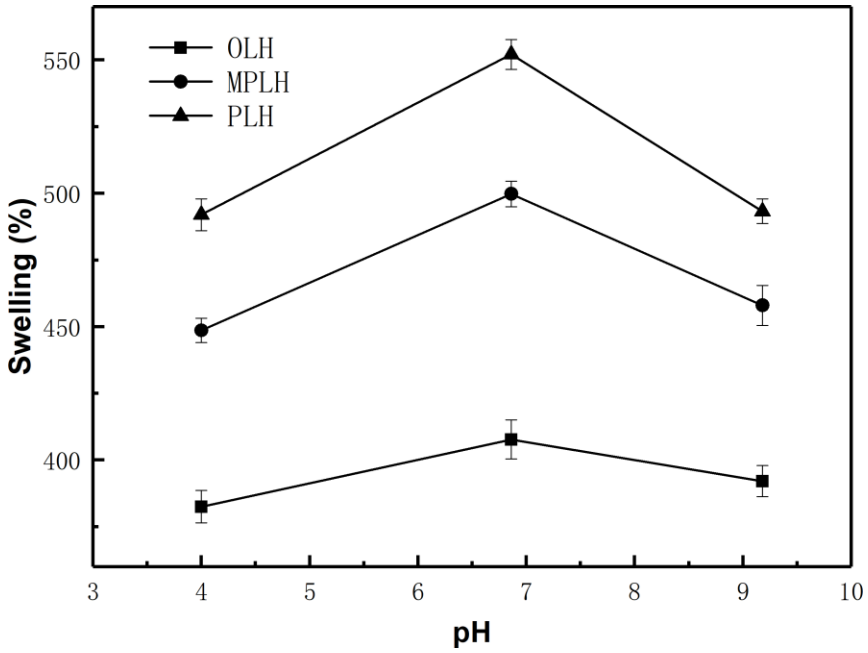

Fig. 7. The swelling of three lignin hydrogels at different pH values

Figure 8 illustrates the responsive time of the three hydrogels tested under the optimum responsive pH of 6.86. From the diagram, the responsive time of PLH was the quickest. Its swelling rate can reached 100% within 13.5 min, which can be explained that the pore size increased owing to the formation of *in situ* voids in the hydrogel and accelerated the swelling rate. The swelling property of MPLH reached 100% at 19.5 min, because the magnetic particles produced by chemical precipitation occupied the original pore space of the hydrogel, and the Fe_3O_4 particles *in situ* also had a certain agglomeration phenomenon. At the same time, the magnetic hydrogel produced in alkaline condition can induce depolymerization, resulting in smaller pore size and lower swelling speed of hydrogel. The pore size of OLH was nanoscale, and its swelling speed and swelling performance were limited, so the swelling time of the hydrogel reached 100% swelling rate within 34 min. Compared to the hydrogels without pore-foaming agent, the degree of swelling increased 47%.

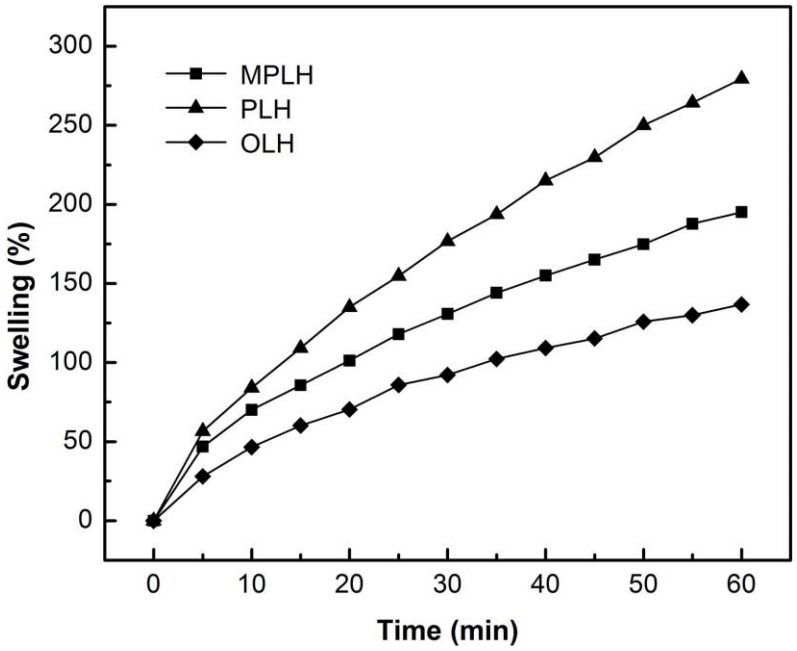

Fig. 8. The swelling of three lignin hydrogels at pH = 6.68

Swelling-deswelling Tests of Hydrogels

The three hydrogels were examined by repeated swelling/deswelling tests to verify their durability. According to Fig. 9, when pH = 6.86 for optimal responsiveness, the swelling property of the PLH hydrogel stayed at the top for 96 h. The PLH hydrogel also showed a remarkable swelling property because of the pore-foaming agent treatment.

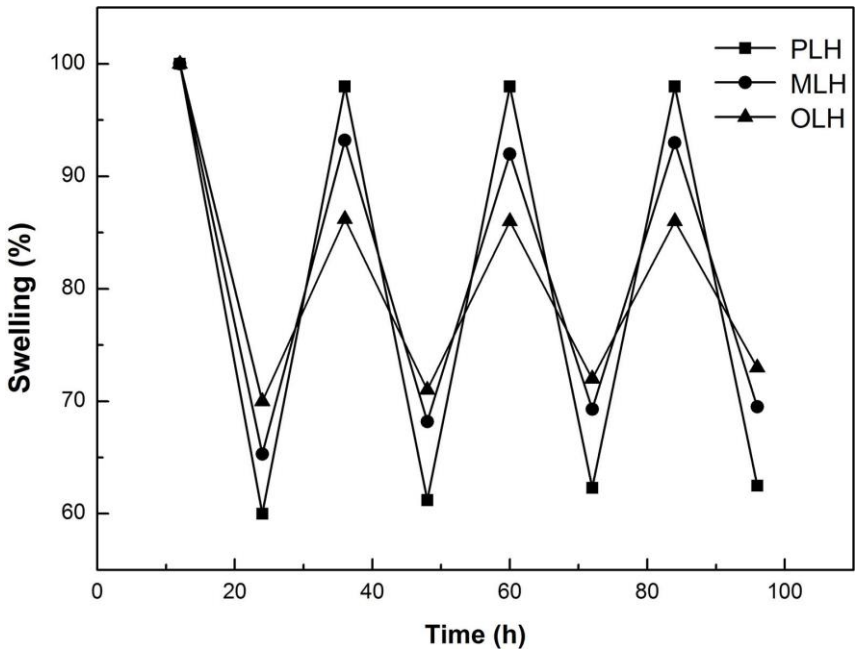

Fig. 9. Swelling-deswelling tests of hydrogels at pH = 6.86

Though the swelling behavior of MPLH hydrogel was slightly inhibited by the blocking and depolymerization effect of generated Fe_3O_4 particles, the overall swelling properties of these three hydrogels stayed at an ideal level. Their absorption capacity did not decrease significantly as the cycles of swelling/deswelling increased, which indicated that hydrogels prepared from the acrylamide matrix showed good durability.

CONCLUSIONS

1. Lignin hydrogels were prepared by free radical polymerization from lignin and acrylamide. Calcium carbonate is an effective pore-foaming agent to improve its swelling properties, Magnetic properties was endowed to the hydrogels by magnetic particles (Fe_3O_4) formed in the polymer by in situ reaction and co-precipitation.
2. The degree of swelling of pH responsive hydrogels (PLH) contained the pore-foaming agent increased 47% compared to the original hydrogels (OLH) without pore-foaming agent, and the swelling rate of PLH reached 100% within 13.5 min under optimum pH conditions (pH = 6.8) which shorten around 1.5 times compare to the OLH. The swelling-deswelling experiments showed that the hydrogels still retained good reversibility and stability.

ACKNOWLEDGEMENTS

This work supported by the National Key R&D Program of China (2017YFD0601004), Scientific Innovation Fund for Post-graduates of Central South University of Forestry and Technology.

REFERENCES CITED

Chen, N., Dempere, L. A., and Tong, Z. (2016). "Synthesis of pH-responsive lignin-based nanocapsules for controlled release of hydrophobic molecules," *ACS Sustain. Chem. Eng.* 4(10), 5204-5211. DOI: 10.1021/acssuschemeng.6b01209

Chung, Y. L., Olsson, J. V., and Li, R. J. (2013). "A renewable lignin–lactide copolymer and application in biobased composites," *ACS Sustain. Chem. Eng*. 1(10), 1231-1238. DOI: 10.1021/sc4000835

Eslahi, N., Abdorahim, M., and Simchi, A. A. (2016). "Smart polymeric hydrogels for cartilage tissue engineering: A review on the chemistry and biological functions," *Biomacromolecules* 17(17), 3441-3463. DOI: 10.1021/acs.biomac.6b01235

Feng, Q., Li, J., Cheng, H., Chen, F., and Xie, Y. (2014). "Synthesis and characterization of porous hydrogel based on lignin and polyacrylamide," *BioResources* 9(3), 4369-4381. DOI: 10.15376/biores.9.3.4369-4381

Gutiérrez-Hernández, J. M., Escalante, A., and Murillovázquez, R. N. J. (2016). "Use of agave tequilana-lignin and zinc oxide nanoparticles for skin photoprotection," *J. Photoch. Photobio. B* 163, 156-161. DOI: 10.1016/j.jphotobiol.2016.08.027

Ji, X., Zhang, Z., Chen, J., Yang, G., Chen, H., and Lucia, L. A. (2017). "Synthesis and characterization of alkali lignin-based hydrogels from ionic liquids," *BioResources* 12(3), 5395-5406. DOI: 10.15376/biores.12.3.5395-5406

Jin, C., Song, W., Liu, T., Xin, J., Hiscox, W. C., Zhang, J., Liu, G., and Kong, Z. (2017). "Temperature and pH responsive hydrogels using methacrylated lignosulfonate cross-linker: synthesis, characterization, and properties," *ACS Sustain. Chem. Eng*. 5 (9), 7502-7506. DOI: 10.1021/acssuschemeng.7b03158

Kai, D., Zhi, W. L., and Liow, S. S. (2015) "Development of lignin supramolecular hydrogels with mechanically responsive and self-healing properties," *ACS Sustain. Chem. Eng.* 3(9), 2160-2169. DOI: 10.1021/acssuschemeng.5b00405

Li, Y. J., Sun, X. F., and Ye, Q. (2014) "Preparation and properties of a novel hemicellulose-based magnetic hydrogel," *ACTA Phys-Chim. Sin.* 30(1), 111-120. DOI: 10.3866/PKU.WHXB201310313

Liu, F., Chen, Y., and Gao, B., J., (2017). "Preparation and characterization of biobased graphene from kraft lignin," *BioResources* 12(3), 6545-6557. DOI: 10.15376/biores.12.3.6545-6557

Liu, N., Huo, K., and McDowell, M. T. (2013) "Rice husks as a sustainable source of nanostructured silicon for high performance Li-ion battery anodes," *Sci. Rep-UK* 3, Article ID 1919. DOI: 10.1038/srep01919

Liu, X. H., Wang, X. G., and Liu, D. S. (2002). "Fast responsive thermosensitive poly (N- isopropylacrylamide) hydrogels I. Synthesis, characterization and kinetic behavior," *ACTA Polym. Sin*. 3(5), 354-357. DOI: 10.3321/j.issn:1000-3304.2002.03.019

Marcelo, G., López-González, M., and Trabado, I. (2016). "Lignin inspired PEG hydrogels for drug delivery," *Materials Today* 7, 73-80. DOI: 10.1016/j.mtcomm.2016.04.004

Mir, N., Bahrami, M., and Safari, E. (2014). "Fluorescent superparamagnetic γ-Fe_2O_3 hollow nanoparticles: Synthesis and surface modification by one-pot co-precipitation method," *J. Clust. Sci*. 26(4), 1103-1113. DOI: 10.1007/s10876-014-0800-7

Nair, V., Panigrahy, A., and Vinu, R. (2014) "Development of novel chitosan–lignin composites for adsorption of dyes and metal ions from wastewater," *Chem. Eng. J.* 254(20), 491-502. DOI: 10.1016/j.cej.2014.05.045

Oroumei, A., Fox, B., and Naebe, M. (2015). "Thermal and rheological characteristics of biobased carbon fiber precursor derived from low molecular weight organosolv lignin," *ACS Sustain. Chem. Eng.* 3(4), 758-769. DOI: 10.1021/acssuschemeng.5b00097

Peng, Y, U., Jiang, C., and Yao, X. J. (2015). "Progress in the application of lignin to the rubber," *Polym. Bull.* 168(3), 26-34. DOI: 10.14028/j.cnki.1003-3726.2015.03.004

Ragauskas, A. J., Beckham, G. T., and Biddy, M. (2014). "Lignin valorization: Improving lignin processing in the biorefinery," *Science* 344(6185), Article ID 1246843. DOI: 10.1126/science.1246843

Ravi, T., and Jabasingh, S. A. (2017). "Preparation and characterization of higher degree−deacetylated chitosan−coated magnetic adsorbent for the removal of chromium(vi) from its aqueous mixture," *Journal of Applied Polymer Science*. 135(9), 12-15. DOI: 10.1002/app.45878

Segtnan, V. H., Kita, A., and Mielnik, M. (2006). "Screening of acrylamide contents in potato crisps using process variable settings and near-infrared spectroscopy," *Mol. Nutr. Food Res.* 50(9), 811-817. DOI: 10.1002/mnfr.200500260

Shen, X., Shamshina, J. L., and Berton, P. (2016). "Comparison of hydrogels prepared with ionic-liquid-isolated *vs* commercial chitin and cellulose," *ACS Sustain. Chem. Eng.* 4(2), 471-480. DOI: 10.1021/acssuschemeng.5b01400

Shen, Z., Luo, Y., and Wang, Q. (2014). "Eu^3+-doped $NaGdF_4$ nanocrystal down-converting layer for efficient dye-sensitized solar cells," *ACS Appl. Mater. Inter.* 6(20), 16147. DOI: 10.1021/am505086e

Song, W., Liu, M., and Hu, R. (2014). "Water-soluble polyacrylamide coated-Fe_3O_4 magnetic composites for high-efficient enrichment of U(VI) from radioactive waste water," *Chem. Eng. J.* 246, 268-276. DOI: 10.1016/j.cej.2014.02.101

Spasojević, D., Zmejkoski, D., and Glamočlija, J. (2016). "Lignin model compound in alginate hydrogel: A strong antimicrobial agent with high potential in wound treatment," *Int. J. Antimicrob. Ag.* 48(6), 732-735. DOI: 10.1016/j.ijantimicag.2016.08.014

Sun, Y., Ma, Y., Fang, G., Ren, S., and Fu, Y. (2016). "Controlled pesticide release from porous composite hydrogels based on lignin and polyacrylic acid," *BioResources* 11(1), 2361-2371. DOI: 10.15376/biores.11.1.2361-2371

Wan, C., and Li, J. (2015) "Facile synthesis of well-dispersed superparamagnetic γ-Fe_2O_3 nanoparticles encapsulated in three-dimensional architectures of cellulose aerogels and their applications for Cr(VI) removal from contaminated water," *ACS Sustain. Chem. Eng.* 3(9), 2142-2150. DOI: 10.1021/acssuschemeng.5b00384

Wang, Y., Xiong, Y., and Wang, J. (2017). "Ultrasonic-assisted fabrication of montmorillonite-lignin hybrid hydrogel: Highly efficient swelling behaviors and super-sorbent for dye removal from wastewater," *Colloid. Surface. A* 520, 903-913. DOI: 10.1016/j.colsurfa.2017.02.050

Xiang, Y., Xu, A., and Zhou, X. (2015) "Research on adsorption of cadmium ions by modified sodium lignosulfonate hydrogel," *Ion Exchange & Adsorption* 31(2), 115-122. DOI: 10.16026/j.cnki.iea.2015020115

Xu, X., Zhou, J., and Nagaraju, D. H. (2015). "Flexible, highly graphitized carbon aerogel based on bacterial cellulose/lignin: Catalyst-free synthesis and its application in energy storage devices," *Adv. Funct. Mater.* 25(21), 3193-3202. DOI: 10.1002/adfm.201500538

Zhang, N. (2012). "Current status and prospect of applied research on lignin," *Chemical Engineer* 26(2), 50-51. DOI: 10.16247/j.cnki.23-1171/tq.2012.02.021

Article submitted: March 11, 2018; Peer review completed: June 5, 2018; Revised version received: August 4, 2018; Accepted: August 6, 2018; Published: August 8, 2018.
DOI: 10.15376/biores.13.4.7281-7293